DTU Library

Twin stability in highly nanotwinned Cu under compression, torsion and tension

Hodge, A.M.; Furnish, T.A.; Shute, C.J.; Liao, Y.; Huang, Xiaoxu; Hong, Chuanshi; Zhu, Y.T.; Barbee Jr., T.W.; Weertman, J.R.

Published in:
Scripta Materialia

Link to article, DOI:
10.1016/j.scriptamat.2012.01.027

Publication date:
2012

Document Version
Early version, also known as pre-print

Preprint
Scripta Materialia 66 (2012) 872–877.
DOI: 10.1016/j.scriptamat.2012.01.027

Twin stability in highly nanotwinned Cu under compression, torsion and tension

A.M. Hodge[a,*], T.A. Furnish[a], C.J. Shute[b], Y. Liao[b], X. Huang[c], C. S. Hong[c] ,Y.T. Zhu[d], T.W. Barbee Jr.[e], JR Weertman [b]

[a]Department of Aerospace and Mechanical Engineering, University of Southern California, Los Angeles, CA 90089, USA

[b]Department of Materials Science and Engineering, Northwestern University, Evanston, IL 60208, USA

[c]RISOE National Laboratory-Danish Technical University, Roskilde, Denmark

[d]Department of Materials Science and Engineering, North Carolina State University, Raleigh, NC 27695, USA

[e]Physical and Life Sciences, Lawrence Livermore National Laboratory, Livermore, CA 94550, USA

*****corresponding author;

AM Hodge Tel: 213-740-4225, email: ahodge@usc.edu

Abstract:

Twin stability under distinct mechanical loads is investigated for highly nanotwinned Cu containing parallel nanotwins~ 40 nm thick. Deformation under compression, torsion, tension and tension-tension fatigue are qualitatively compared in order to assess twin stability as a function of the loading direction and stress. It is observed that the twins are very stable although microstructural changes vary with deformation mode. Deformation-induced grain growth, shear bands and detwinning are also discussed.

Keywords: nanotwinned, copper, plastic deformation, nanostructure

Preprint
Scripta Materialia 66 (2012) 872–877.
DOI: 10.1016/j.scriptamat.2012.01.027

1. Introduction

Highly nanotwinned (nt) materials have shown great potential as an alternative to nanocrystalline metals [1]. It has been found that nt metals have a strength comparable to that of nanocrystalline (nc) metals, with twin boundary (TB) spacing playing the role of the grain size [2-4]. Hall-Petch plots of the yield strength of nc Cu vs. grain size have been observed to lie on roughly the same line as that for nt Cu vs. TB spacing. However nc metals are quite brittle [5], while nt Cu has a notably higher ductility [2].

Another important advantage of the nt microstructure is its stability as compared to nc metals, which have been found to undergo extensive and rapid grain growth under stress [6, 7]. Twin stability is highly correlated to the role of twin boundaries and the mechanisms which allow TBs to move, thereby causing twins to grow or shrink (and even disappear) [8-10]. The TBs offer a strong barrier to dislocation motion but mechanisms exist to permit their motion. An important mechanism for the growth or shrinkage of a twin/matrix is the glide motion along the TB interface of Shockley partial dislocations under external stress [e.g.,[2, 11]. The dislocations may be grouped to form incoherent twin boundaries (ITBs) which form ledges on the TBs [9, 12]. The extensive glide of individual partial Shockley dislocations or ledges can lead to the disappearance of a twin or matrix and growth of its neighbor. (In the initial microstructure, the distinction of which grains are called twins and which matrix is arbitrary)

Therefore, in the present paper we examine the effects of various forms of deformation on twin stability in Cu samples containing parallel columns of highly aligned nanotwins. The

Preprint
Scripta Materialia 66 (2012) 872–877.
DOI: 10.1016/j.scriptamat.2012.01.027

comparison is qualitative in nature. The magnitude of the applied stresses/strains varies but all are large: almost 2 GPa in the case of compression, a significant fraction of a GPa for tension and tension-tension tests, and shear strains of the order of 1 to 20 imposed by high pressure torsion (HPT). However imperfect the matching, these tests reveal differences and similarities in the effect of various forms of deformation which are oriented in different directions with respect to the TBs. Here the term "detwinning" refers to the disappearance of the original nanotwinned structure which may be replaced by a single grain or by a new twin structure with TBs in a different orientation and/or with different TB spacing. Thus, microstructural stability will be correlated to observations or lack therefore of detwinning in the microstructure.

2. Experimental Procedures

High-purity (99.999%+) Cu foils were deposited onto (100) silicon wafers by interrupted d.c. magnetron sputtering, following the procedures described in previous publications [13, 14]. The films, approximately 170 µm thick, were ''freely" removed from the substrate and were handled as free-standing foils. The initial microstructure consists of columns, parallel to the growth direction, of aligned twins separated by parallel coherent Σ3 interfaces. The columns are ~ 500 – 800 nm wide; the initial twin spacing, which is highly variable, has a median value of 35 – 40 nm [13, 14]. Compression, torsion, tension, and tension-tension fatigue tests were performed at room temperature using a variety of equipment, as described in previous publications [12, 15-17]. For the different tests the samples were loaded as shown in **Fig. 1,** which also shows the initial orientation of the twinned microstructure. In the following sections we discuss the effect of each of the different types of deformation on the stability of the nanotwinned microstructure.

Preprint
Scripta Materialia 66 (2012) 872–877.
DOI: 10.1016/j.scriptamat.2012.01.027

3. Results and Discussion

3.1. Deformation by compressive stress

In this section the sample was loaded as shown in Figure 1a. Specifically, a polished and lubricated disk of 3 mm diameter was compressed under a stress of 1800 MPa [17]. As a result the thickness of the disk decreased to 0.78 of the original value, corresponding to a negative strain in the axial direction of 25%. FIB and TEM images show little to no loss of twins, and in general the column boundaries remain parallel to the growth direction and are only slightly rough (Fig 2a). The initial median TB spacing of 35-40 nm drops to ~ 25 nm, roughly the drop expected from the negative strain in the axial direction.

However in a number of cases columns are seen to become increasingly narrow and truncated. An example is shown in **Fig. 2a**. These truncation sites may become high stress regions under the applied compressive stress, as noted by a strong dislocation presence (Fig. 2b). The TB spacing in the immediate region increases notably (**in Fig. 2b** to 45 nm or even greater, from a post-strain median value of ~ 25 nm in most other regions of the sample). The increase in TB spacing and deviation of some of the column boundaries from their original location parallel to the growth direction are consistent with the motion of Shockley partial dislocations forming ledges gliding on twin boundaries, as described by Wang et al. [9].

3.2 Deformation by shear stress

In this section the sample deformed as shown in Figure 1b. The effect of a shear strain parallel to the twin boundaries was examined through high pressure torsion (HPT). The first indication

Preprint
Scripta Materialia 66 (2012) 872–877.
DOI: 10.1016/j.scriptamat.2012.01.027

of the importance of shear deformation on the twinned microstructure came from indentation tests [16]. Shear bands were seen parallel to the face of the indenter, and are interpreted as the result of shear stress on the nanotwinned samples from the Vickers indenter. Focused Ion Beam (FIB) images showed that the shear bands consisted of strings of nanocrystalline grains, which represents a form of detwinning.

To further explore the effect of shear stress, polished disks 10 mm in diameter and 150 µm in thickness were subject to HPT deformation of a 180° twist under a 3 GPa compressive stress between flat anvils. The deformed samples were examined at 1 mm from the center of rotation (see ref. [15] for details of the HPT experiments). The FIB cuts and TEM foils were oriented in the direction of maximum shear strain. F**igure 3a** shows a FIB image of a transverse cut starting at the sample surface and going some 20 µm into the interior. It can be seen that there is a narrow layer of very fine grains at the surface that is abruptly replaced by large “grains” that follow a twisting pattern ending in columns of the original twins. The overall shear strain sustained by the disk is 21 [15], but as seen in Fig. 4 of ref [4], the shear strain in the sample is a strong function of depth. At the surface the shear strain is extremely high, it drops to about 6 at the onset of the large grains, and is estimated to be about 1 where the twins first appear and 0.6 at the center of the sample.

Original TEM measurements indicated that the individual large grains are single crystals but later, very careful TEM measurements showed that these features are still twinned, if somewhat sparsely (**Figs. 3b,c).** Selected Area Diffraction (SAD) shows a near perfect twin-matrix relationship. The wedge-shaped appearance of the twin lamella suggests their shrinking behavior by detwinning, likely by the motion of Shockley partial dislocations gliding along the TBs under the applied shear stress [2, 9, 11, 12]. The rounded shape of the left side of the matrix is the boundary of a "large grain", which has twisted from the original orientation parallel to the surface, as seen in Fig. 3a and Fig. 1 in Ref. [15]. However the TBs have remained roughly parallel to the sample surface. Evidently some twinning structure persists at strains even higher than 1. In the region where the nt structure is largely retained (lower portion of Fig. 3a), there is some disappearance of the original nanotwins; however, it is generally confined to individual columns (seen in Fig. 3d).

3.3 **Deformation by tensile stress**

In this section the samples are loaded as shown in Figure 1c using dogbone-shaped samples with a gage length of ~ 6 mm by 3 mm width under different testing procedures.

3.3.1 *Tensile Tests*

Tensile tests were performed at a strain rate of 10^{-4} /s. Figure **4a** shows a representative optical micrograph of the gage section after fracture. In a recent study by Hodge et al, the microstructures at various locations within a fractured nt tensile sample tested at room temperature were shown to maintain the highly nt structures, even within the areas of highest deformation [12]. In this study, we go a step further by focusing on the regions near the fractured edge (black box in Fig. 4a), in which regularly spaced surface depression lines (vertical lines in Fig. 4b) are observed running parallel to the fractured edge (right side of Fig. 4b). In the center of Fig. 4b, a FIB trench prepared for cross-section imaging is shown centered across a depression line that is approximately 30μm away from the edge. In **Figure 4c**, the micrograph depicts a detwinned nanograin structure (highlighted by the black rectangle) which can clearly be observed under the surface depression. A representative micrograph of the nanograined structure can be seen in **Fig. 4d.** It should be mentioned that FIB cross-section analysis was also done

Scripta Materialia 66 (2012) 872–877.
DOI: 10.1016/j.scriptamat.2012.01.027

directly along the fractured edge (within 1μm from the edge) and the same nanograined-type structure was observed. It is interesting to note that on either side of the nanograined regions (in between the surface depression lines), the nanotwins are mostly intact, and that the main changes in the microstructure is a stretching/blending of the columnar grains coupled with twin misregistry on either side of the boundaries. Similar observations were made by Shute et al in which a sample fatigued between 450 and 45MPa to failure showed a nanocrystalline grain structure underneath surface dips, while the majority of twins outside of the dips survived with approximately their original orientation [17].

In order to further explore the microstructural stability of the nt samples and the role of nt's in the observed localized plastic deformation, a tensile test of the nt-Cu (strain rate of 10^{-4}/s) was stopped immediately after the yield peak. **Figure 5a** shows an optical micrograph of the gage section after the test was stopped, in which a clear shear band is observed across the entire width. A slight difference in the surface roughness is observed in the magnified micrograph in Figure **5b**. A representative cross-section FIB micrograph within the shear band region is shown in **Figure 5c**, in which there is little to no change in the microstructure compared to the as-prepared sample. It should be mentioned that FIB cross-section analysis of the microstructure was done in multiple locations within the shear band region and at various orientations relative to the shear band direction. In all cases, the microstructure was similar to that seen in **Fig. 5c**. This observation implies that the shear band was formed prior to any major change in microstructure, such as grain growth or detwinning. This result is in contrast to TEM observations by Hong et al [11], in which shear bands in a Cu-Al alloy processed by dynamic plastic deformation were seen to form as a result of bending, necking, and then detwinning of the original twin/matrix lamella.

Preprint
Scripta Materialia 66 (2012) 872–877.
DOI: 10.1016/j.scriptamat.2012.01.027

However, the current study is a report on growth twins, rather than deformation twins, and in addition very minor changes in the twin structure are beyond the FIB resolution.

3.3.2 Tension-tension cycling

Deformation by tension-tension fatigue permits the study of accumulated strain on the nt microstructure. Stresses are applied in the same direction as in the case of the tension tests, but by cycling through several thousand cycles, the microstructure is subjected to a large accumulated strain, far greater than the fracture strain in a tension test. It is seen that fatiguing to failure in the low cycle regime produces a change in the nanotwinned microstructure (See refs [16, 17]). While most of the original twins remain, column boundaries are disturbed and within a number of columns, the original nanotwins have been replaced by other twins having different twin boundary spacing and orientation (**Fig. 6a**, see also Fig.3c in ref [16]). Damage originates at the surface, as is generally the case in fatigue failures. An SEM image (Fig. 6b) of the surface of a sample cycled between 550 and 55 MPa to failure at ~4000 cycles shows parallel depressions, crossing the surface at an angle of roughly 30° to the tensile stress direction. The image was taken about 1 mm away from the fracture site. These lines become more apparent as the fracture edge is approached. Closer to the fracture another set of parallel lines appears, slanted in the opposite direction (see Fig.7a in [17]). (This second set of lines might have been present but not apparent in Fig. 6b because of the tilt of the sample during imaging.) Surface cracks tend to appear at the intersection of two lines from the opposite sets (Fig 6c). A FIB image (Fig. 6d) of a cut made transverse to one of the lines near the fracture site in the sample fatigued between 550 and 55 MPa shows some loss of the original nanotwins near the surface, which has dipped below its original position. This loss of the original nanotwins at the surface under a surface depression line is similar to the damage seen in the tensile test, Fig 4c.(See also Fig. 6 in [17]). In all of these figures the loss of original twinning is confined to a few µm at the surface.

4. Summary and Conclusions

Samples of Cu containing highly aligned nanotwins have been deformed in four different configurations. In all cases the magnitude of the stresses, while differing from test to test, were large. To a significant extent the nanotwin structure survived the deformations. However differences exist in the resultant changes to the microstructure. The nanotwinned microstructure under *compression* is very stable under a high stress perpendicular to the TBs. Essentially no change was seen in the hardness (i.e., yield strength) as a result of the compression [17].

In the *torsion experiments*, a strong shear strain in the direction of the TBs has been shown to affect the twinned microstructure, either destroying it altogether by intense grain refinement near the sample surface, or else changing the original twins into grains. However the original columns of twins in the sample interiors have persisted even up to the high shear strain of 1, and evidence of persistent twinning in the grains is seen at even higher shear strains.

In the *tension tests* detwinned nanograined structures were only seen to form within observed surface depression lines near the fractured surface and along the actual fractured edge. The nt structure was overall very stable, even near the nanograined regions. In addition, there was no noticeable change in the nt spacing or the TBs orientations within the non-fractured shear bands, indicating that the shear bands were formed prior to the detwinned nanograined structure.

Tension-tension cycling in the low cycle regime (failure in the several thousand cycles) with the stress direction parallel to the TBs, leads to a significant change in the nanotwinned microstructure, particularly in the general vicinity of the fracture site. Column boundaries are disturbed and within many columns the original nanotwinned structure has been replaced by twins with TBs with different spacing and oriented in a new direction. The hardness has decreased by about 12 % [17]. Surface depressions form on the surface, as in the case of the tension tests, but distributed over a wider distance from the fracture. These are sites for damage in the form of surface cracks that originate in the subsurface region where loss of the original nanotwin structure occurred.

Acknowledgements

Parts of his work were performed under the auspices of the U. S. Department of Energy at Lawrence Livermore National Laboratory under Contract DE-AC52-07NA27344, at USC under NSF grant number DMR-0955338. At Northwestern University, shared facilities at the Materials Research Center were used supported by the MRSEC Program of the National Science Foundation (DMR-020513).

Preprint
Scripta Materialia 66 (2012) 872–877.
DOI: 10.1016/j.scriptamat.2012.01.027

Figure captions

Figure 1. Schematic of tests setup with respect to grain and twin orientation for a) compression, b) torsion and c) tension.

Fig. 2a. FIB image of a nanotwinned Cu sample after deformation under a compressive stress of 1800 MPa. Note truncated column of twins. (b) TEM image of a high stress region in a column boundary region of sample in (a).

Figure 3. (a) FIB image of a transverse cut of nanotwinned sample subjected to a half turn, 1 mm from the center of rotation, oriented for maximum shear stress. (b) and (c) Dark field images of twins and matrix in a large grain located near the boundary with the fine grain structure [15]. The TBs remain approximately parallel to the sample surface. (d) Columns of nanotwins in the sample interior on either side of a column that has lost its original nanotwin structure.

Figure 4. (a) Optical micrograph of a gage section after fracture of a representative tensile sample tested at 10^{-4}/s. (b) Planar view of the FIB trench prepared for cross-section imaging. (c) FIB cross-section centered at the trench where a surface depression line near the fractured edge shows detwinning (d) representative magnified FIB image of a detwinned region.

Figure 5. (a) Optical micrograph of the gage section of a representative tensile sample tested at 10^{-4}/s that was stopped immediately after the yield peak in the stress-strain curve. (b) A magnified optical micrograph of the shear band across the specimen width. (c) FIB cross-section micrograph of a section within the shear band region [location of FIB cut marked by double-headed arrow in (b)].

Figure 6. (a) Transverse cut of a nanotwinned Cu sample that has been fatigued to failure under a stress of 450 MPa. (Cut taken close to fracture site). (b) SEM image of surface of sample fatigued to failure at ~4000 cycles under a maximum stress of 550 MPa. Image is taken about 1 mm from the fracture site. Note the depression lines crossing the surface. (c) SEM of the surface of a sample fatigued to failure under a maximum stress of 405 MPa, showing apparent damage sites. Image is near the fracture site. (d) FIB image of a cut across a shear band in sample fatigued to failure under a maximum stress of 550 MPa, image taken near failure site. Note that the original nanotwinned structure has been lost in the region of the surface dip.

References

[1] K. Lu, L. Lu, S. Suresh, Science, 324 (2009) 349-352.
[2] M. Dao, L. Lu, Y.F. Shen, S. Suresh, Acta Materialia, 54 (2006) 5421-5432.
[3] L. Lu, X. Chen, X. Huang, K. Lu, Science, 323 (2009) 607-610.
[4] L.L. Shaw, A.L. Ortiz, J.C. Villegas, Scr. Mater., 58 (2008) 951-954.
[5] K.S. Kumar, H. Van Swygenhoven, S. Suresh, Acta Materialia, 51 (2003) 5743-5774.
[6] M. Jin, A.M. Minor, E.A. Stach, J.W. Morris, Acta Materialia, 52 (2004) 5381-5387.
[7] K. Zhang, J.R. Weertman, J.A. Eastman, Appl. Phys. Lett., 87 (2005).
[8] A.G. Frøseth, P.M. Derlet, H.V. Swygenhoven, Grown-in twin boundaries affecting deformation mechanisms in nc-metals, AIP, 2004.
[9] J. Wang, N. Li, O. Anderoglu, X. Zhang, A. Misra, J.Y. Huang, J.P. Hirth, Acta Materialia, 58 (2010) 2262-2270.
[10] Z.H. Jin, P. Gumbsch, E. Ma, K. Albe, K. Lu, H. Hahn, H. Gleiter, Scr. Mater., 54 (2006) 1163-1168.
[11] C.S. Hong, N.R. Tao, X. Huang, K. Lu, Acta Materialia, 58 (2010) 3106-3116.
[12] A.M. Hodge, T.A. Furnish, A.A. Navid, T.W. Barbee Jr, Scr. Mater., 65 (2011) 1006-1009.
[13] A.M. Hodge, Y.M. Wang, T.W. Barbee Jr., Materials Science and Engineering, 429A (2006) 272-276.
[14] A.M. Hodge, Y.M. Wang, T.W. Barbee, Scr. Mater., 59 (2008) 163-166.
[15] C.J. Shute, B.D. Myers, Y. Liao, S.Y. Li, A.M. Hodge, T.W. Barbee Jr, Y.T. Zhu, J.R. Weertman, Scr. Mater., 65 (2011) 899-902.
[16] C.J. Shute, B.D. Myers, S. Xie, T.W. Barbee, A.M. Hodge, J.R. Weertman, Scr. Mater., 60 (2009) 1073-1077.
[17] C.J. Shute, B.D. Myers, S. Xie, S.Y. Li, T.W. Barbee Jr, A.M. Hodge, J.R. Weertman, Acta Materialia, 59 (2011) 4569-4577.

Figure 1

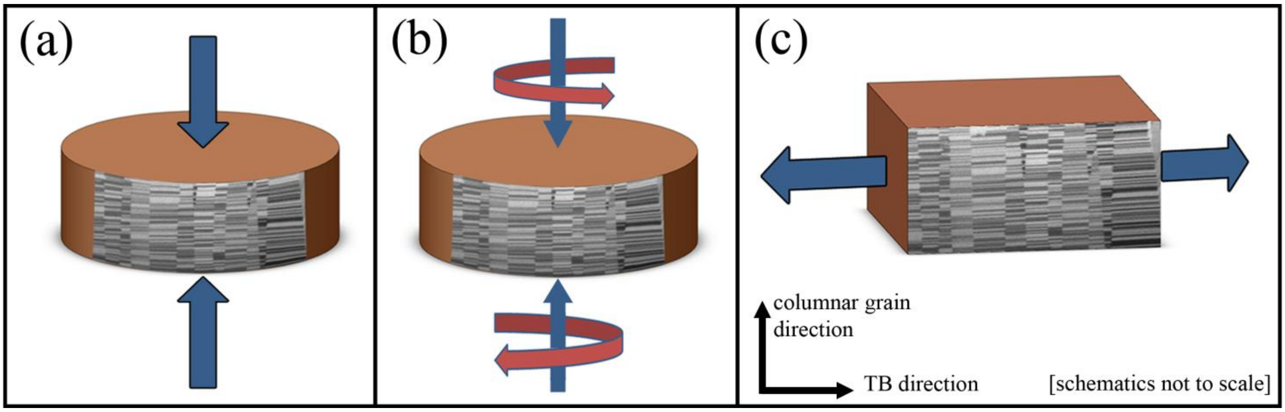

(a)
(b)
(c)
columnar grain
direction
TB direction
[schematics not to scale]

Figure 2

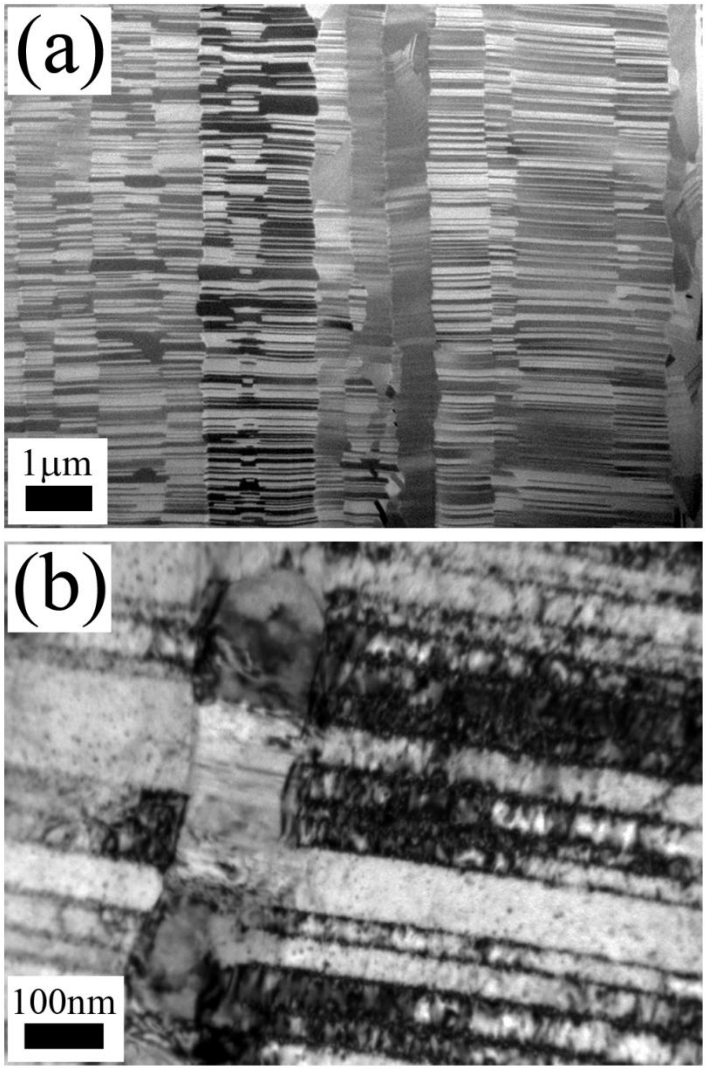

Figure 3

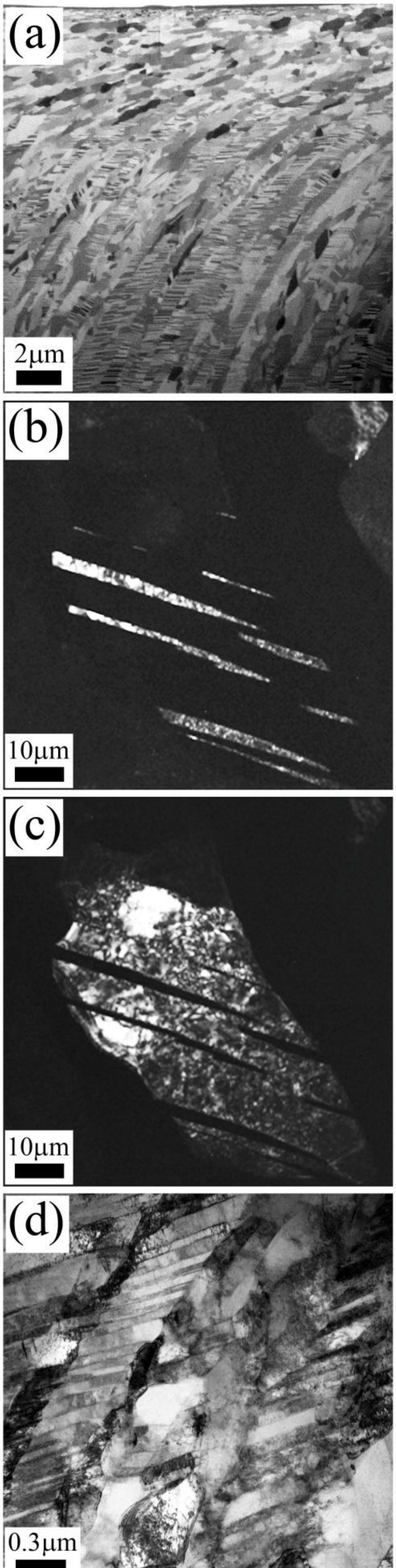

Figure 4

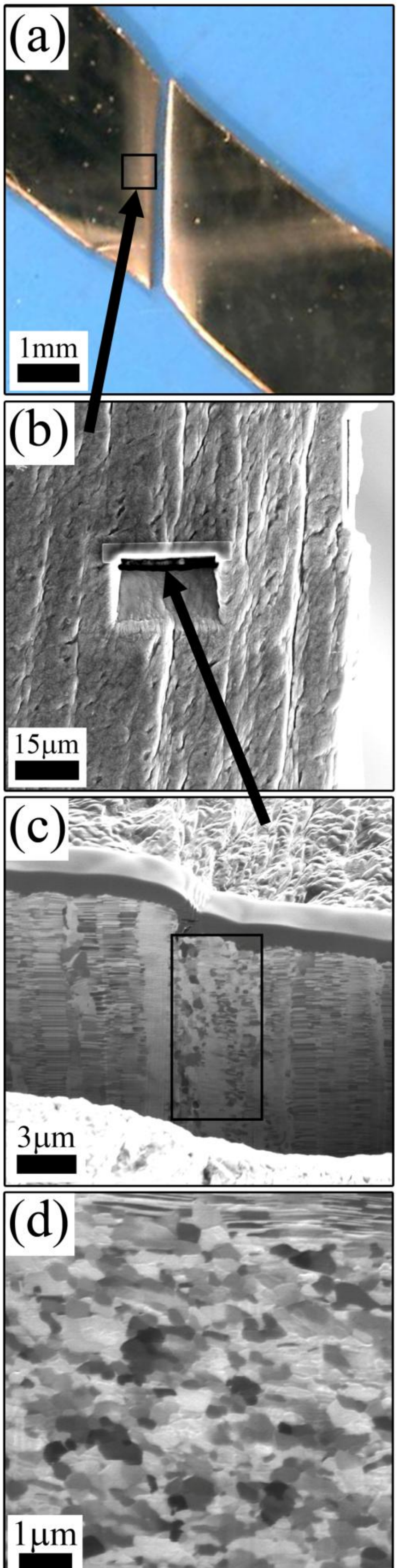

Figure 5

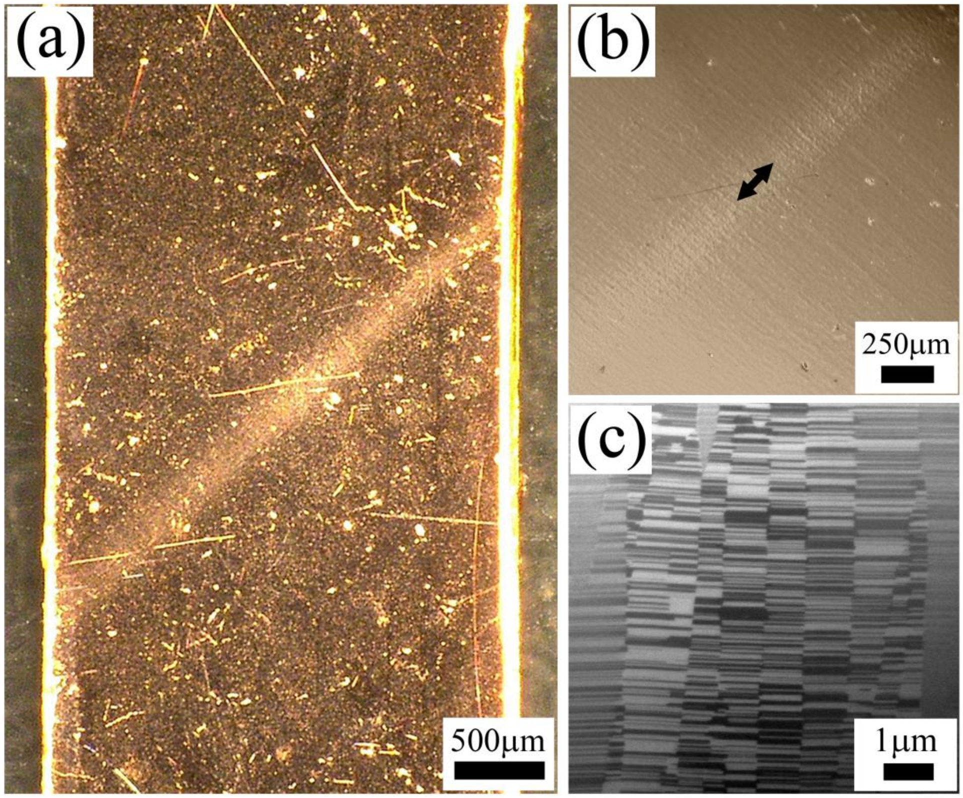

Figure 6